

Supplemental Material Table of Contents

Supplemental Methods

Supplemental References

Supplemental Figures

Supplemental Figure 1. Additional phenotypic characterization of *Pkhd1-Pkd1* mutant mice

Supplemental Figure 2. The *Pkhd1-Pkd1* genetic interaction is dosage dependent

Supplemental Figure 3. Characterization of *Pkd1* mutant rats

Supplemental Figure 4. FPC expression and maturation is tightly regulated

Supplemental Figure 5. Additional analysis of DEG profiles

Supplemental Tables

Supplemental Table 1. Sexual dimorphism in renal phenotype

Supplemental Table 2. Animals used in RNAseq analysis

Supplemental Table 3. Differential expressed genes in *Pkhd1*^{-/-}, *Pkd1*^{RC/RC} and digenic kidneys (Attached separately)

Supplemental Table 4. *Pkhd1*^{-/-}, *Pkd1*^{RC/RC} and digenic gene set enrichment analysis

Supplemental Table 5. Merged cilia-associated annotated gene list from Gene Ontology Consortium

Supplemental Methods

Generation of Pkd1 rat model. *Pkd1* mutant rats (LEW-*Pkd1*^{em6M_{cwi}}; RGDID: 10054439) were produced by TALEN mutagenesis. Messenger RNAs (5ng/uL each) encoding TALENS targeting the *Pkd1* exon 29 target sequence 5'- ATGGGACAGGCCACCTCGTAG[CCGCTTTA]CTAGAGTCCAGAGGGTT-3' were injected into the pronucleus of Lew/NCrl (Charles River Laboratories) rat embryos. Individual TALEN monomer binding sites are underlined. Founder animals were screened using the Cel-I nuclease assay as previously described² and a founder animal harboring an 8-bp deletion mutation (CCGCTTTA) in exon 29 (bracketed in the target sequence above) was identified by Sanger sequencing (not shown). This founder was backcrossed to the parental Lew/NCrl strain and subsequent litters were genotyped by fragment analysis³ using fluorescently-labeled M13-tagged primers Pkd1_F: 5'-M13-CAGTGACGGGCGGTTCACTG-3' and Pkd1_R: 5'-CCTTACTCCGGGACATCCGG-3'.

Blood urea nitrogen measures. Blood was collected from rats at time of sacrifice via cardiac puncture and blood plasma isolated by centrifugation for 15min at 1,500 rpms. BUN levels were measured in duplicate from 1:2 diluted plasma using Quantichrome urea assay kits (Bioassay Systems, Cat#DIUR-100) according to the **protocol**.

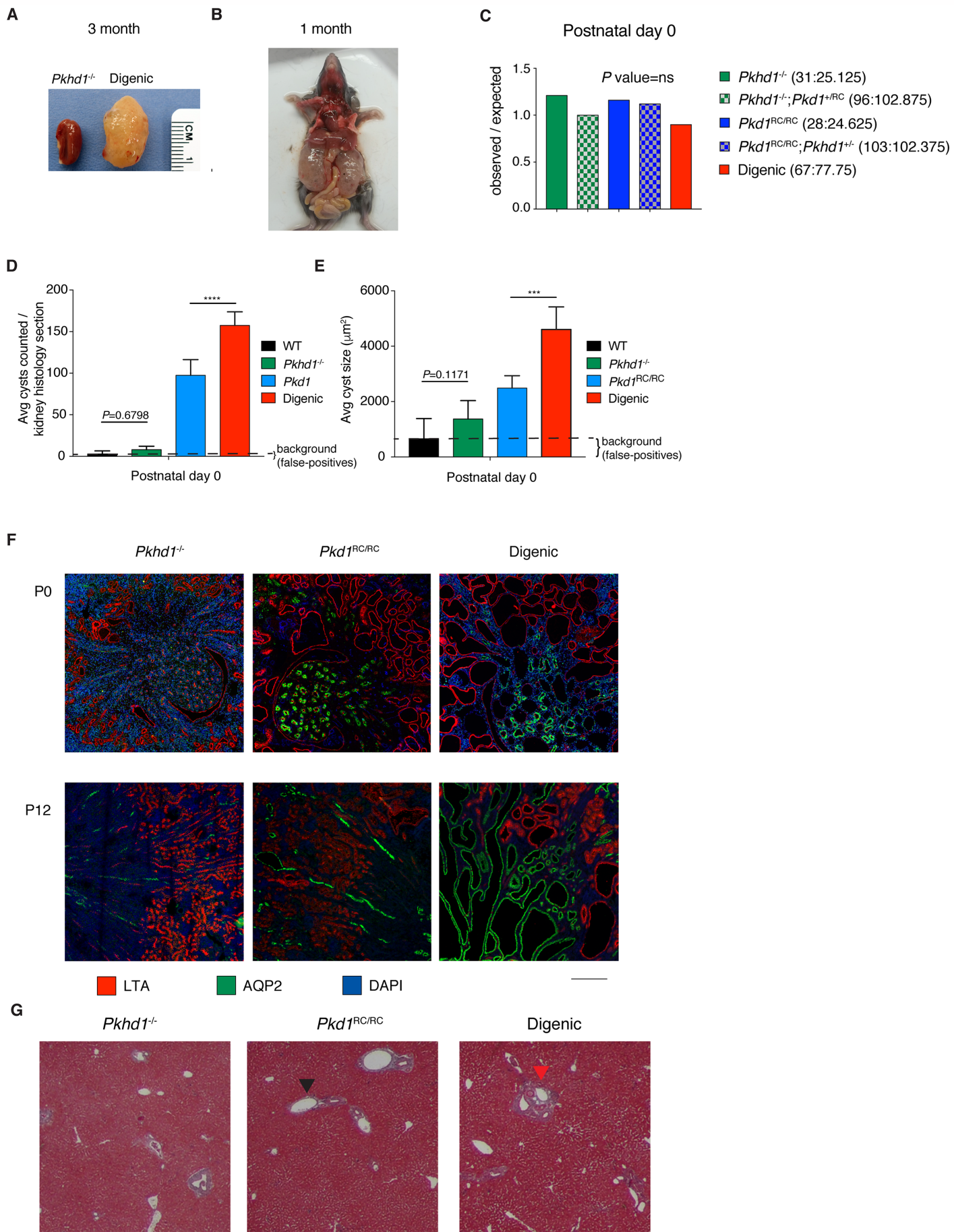
IF labeling. Tissues were prepared for IF labeling as previously described. Biotinylated-LTA (1:250, Vector Laboratories) and rabbit anti-AQP2 (1:1000, ProSci Cat#7621) were used to label proximal tubules and collecting ducts, respectively. DAPI was used to counterstain nuclei.

Supplemental References

1. Jat, PS, Noble, MD, Ataliotis, P, Tanaka, Y, Yannoutsos, N, Larsen, L, Kioussis, D: Direct derivation of conditionally immortal cell lines from an H-2Kb-tsA58 transgenic mouse. *Proc Natl Acad Sci U S A*, 88: 5096-5100, 1991.
2. Geurts, AM, Cost, GJ, Remy, S, Cui, X, Tesson, L, Usal, C, Menoret, S, Jacob, HJ, Anegon, I, Buelow, R: Generation of gene-specific mutated rats using zinc-finger nucleases. *Methods Mol Biol*, 597: 211-225, 2010.
3. Moreno, C, Kennedy, K, Andrae, JW, Jacob, HJ: Genome-wide scanning with SSLPs in the rat. *Methods Mol Med*, 108: 131-138, 2005.
4. Eden, E, Navon, R, Steinfeld, I, Lipson, D, Yakhini, Z: GOrilla: a tool for discovery and visualization of enriched GO terms in ranked gene lists. *BMC Bioinformatics*, 10: 48, 2009.
5. Eden, E, Lipson, D, Yogev, S, Yakhini, Z: Discovering motifs in ranked lists of DNA sequences. *PLoS Comput Biol*, 3: 508-522, 2007.

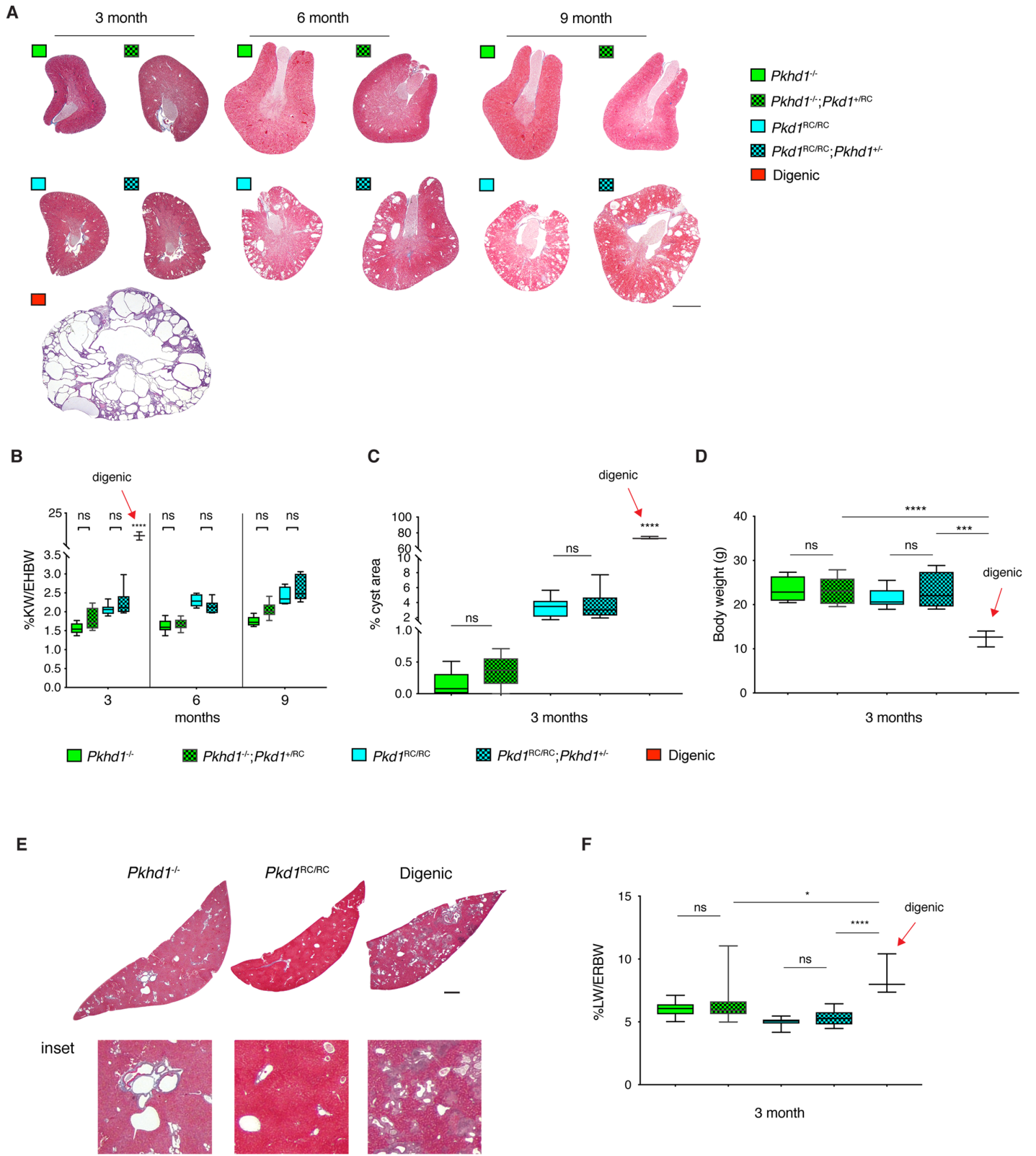
Supplemental Figures

Supp Fig 1



Supplemental Figure 1. Additional phenotypic characterization of *Pkhd1*-*Pkd1* mutant mice. (A-B) Picture of excised digenic and *Pkhd1*^{-/-} kidneys from mice aged to 3 months (A) or 1m old digenic mouse with exposed thoracic and abdominal cavity (B), illustrating the severity of the disease. (C) Analysis of number of animals born vs expected (observed/expected) shows that the digenic animals are not significantly underrepresented at P0 ($P=0.6338$). (D) Cyst number ($\geq 500\mu\text{m}^2$) and (E) average cyst area of the homozygous and digenic genotypes at P0. Digenic kidneys were more severely affected than *Pkd1*^{RC/RC}. Note, there was a slight increase, albeit insignificant, in cystic lesions in *Pkhd1*^{-/-} kidneys compared to WT controls. Values were obtained from analysis of a single histological section taken from 5 mice per genotype. (F) IF labeling of kidney sections from P0 and P12 *Pkhd1*^{-/-}, *Pkd1*^{RC/RC} and digenic mice. Proximal tubules (PT) were stained with the lectin LTA (red) and collecting-ducts (CD) with an antibody to AQP2 (green), and counterstained with DAPI, 10x magnification. Scale bar = 200 μm . (G) Masson's Trichrome stained section of P12 *Pkhd1*^{-/-}, *Pkd1*^{RC/RC} and digenic livers. Black arrow denotes normal ductal plate and red arrow denotes ductal plate malformation. Scale bar=200 μm . Statistical values were obtained by Chi square analysis or one-way ANOVA, followed by Tukey's multiple comparisons test where appropriate ($*P < 0.05$, $**P < 0.01$, $***P < 0.001$, $****P < 0.0001$); error bars indicate $\pm\text{SD}$.

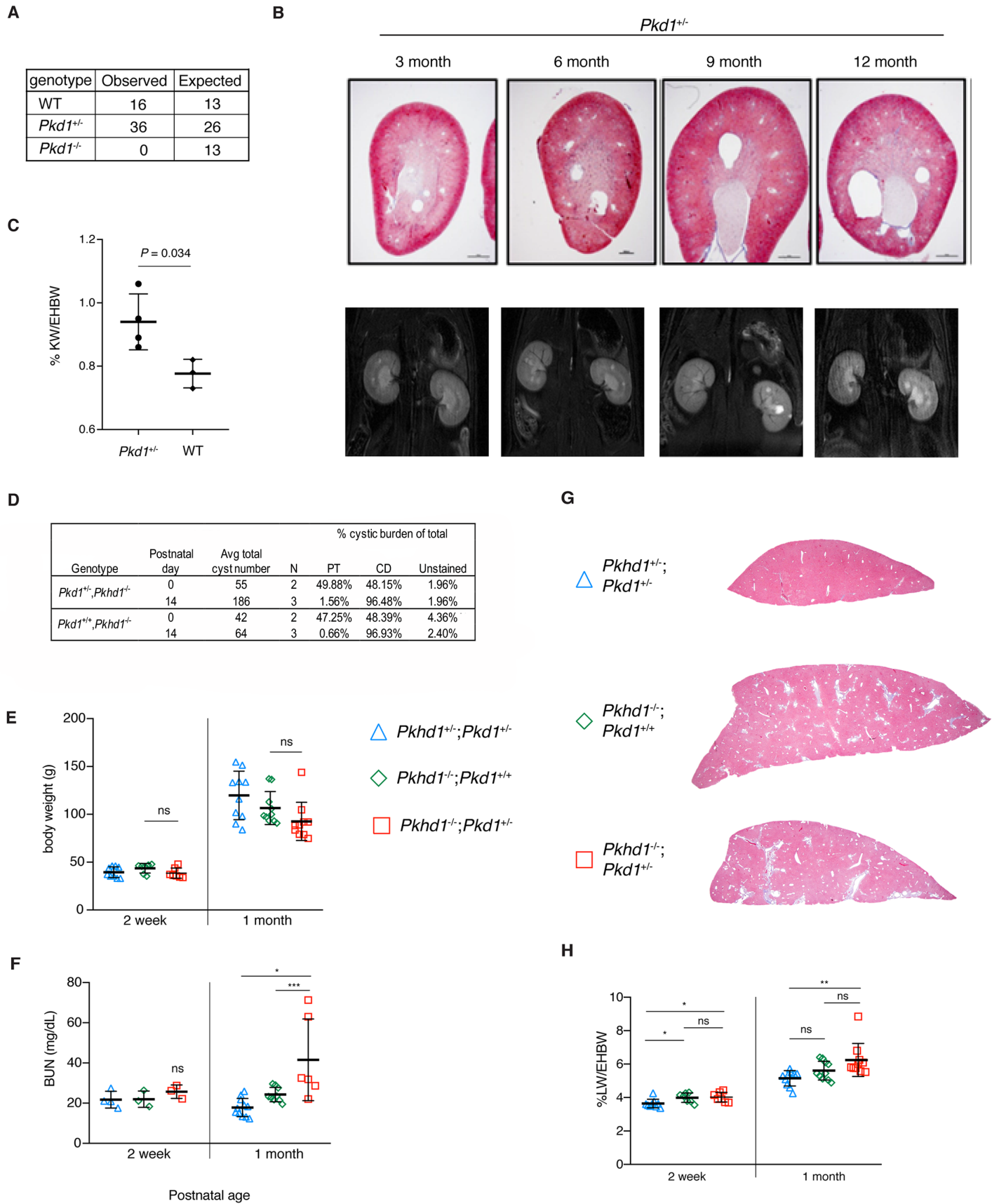
Supp Fig 2



Supplemental Figure 2. The *Pkhd1*-*Pkd1* genetic interaction is dosage dependent. (A) Representative Masson's Trichrome stained kidney sections from the five different genotypes at 3m, and 6 and 9m, without

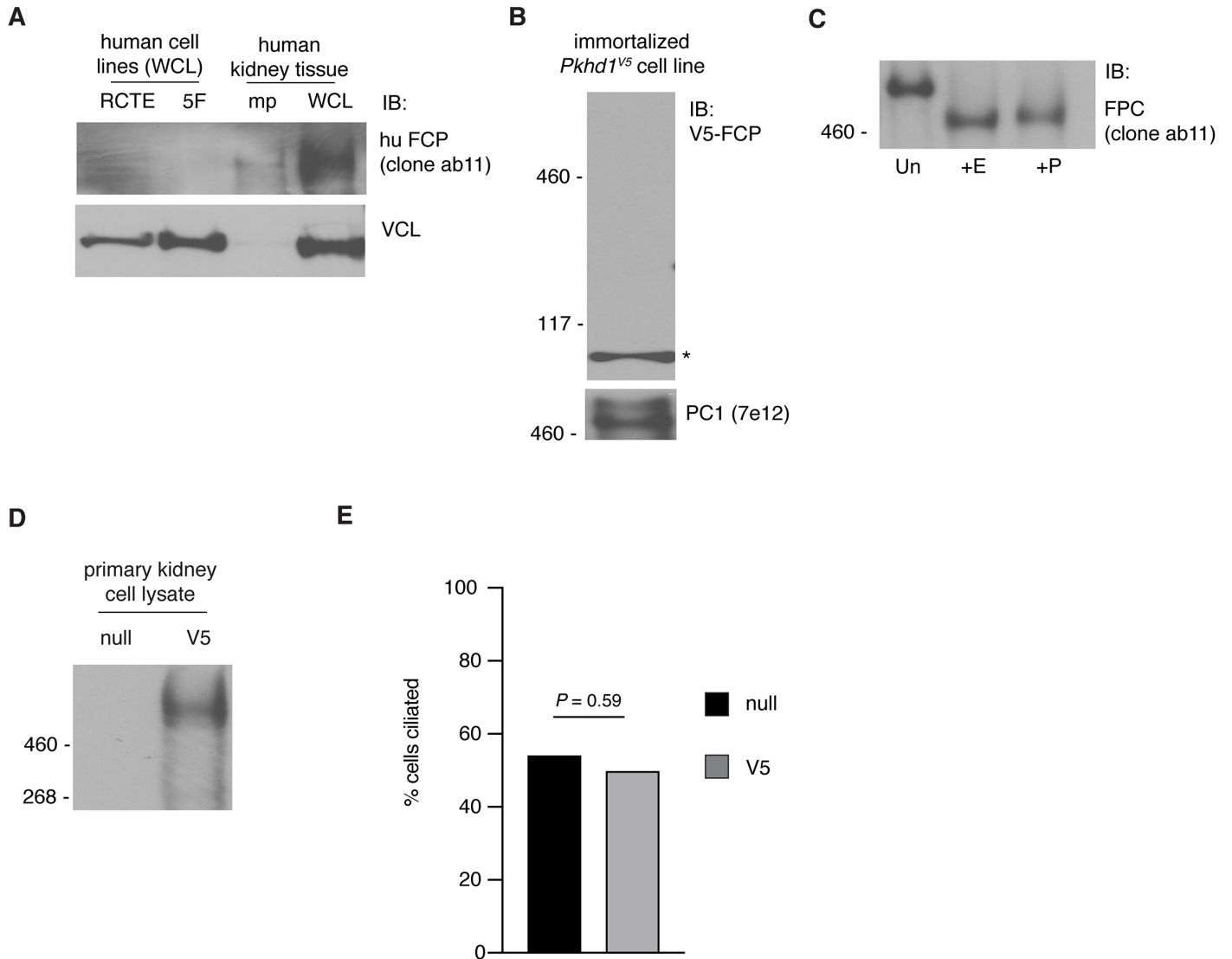
digenic kidneys as no animals survived past 3m. The synergist interaction in the digenic animals is clearly shown with the hugely enlarged kidney. Scale bar = 1mm. (B) Graphical representation of %KW/EHBW at 3, 6 and 9m showing that addition of a single allele of the other genotype ($Pkd1^{+/RC}$ plus $Pkhd1^{-/-}$ or $Pkhd1^{+/-}$ plus $Pkd1^{RC/RC}$) is not sufficient to modify the kidney disease, whereas digenic mice have greatly enlarged kidneys at 3m. Liver weight was subtracted from gross body weight as $Pkhd1^{-/-}$ animals present significant gross enlargement in liver disease by 6m (data not shown). (C) Cyst kidney area, as a percentage of total kidney area, at 3m compares the five genotypic groups (n=10 per genotype, with the exception of digenic [n=3]). (D) Body weight (g) of mutant mice at 3m showing that only digenic mice have significant growth retardation, confounding the KW/EHBW measurements. (E) Masson's Trichrome sections of liver histology showing a significant increase of ductal plate malformation and fibrosis by 3m in digenic mice compared to the homozygous animals. Scale bar = 500 μ m liver cross-section; 150 μ m inset. (F) Percent liver weight per ex-renal body weight (%LW/ERBW) of the various genotypes at 3m showing a significant increase in the digenic animals. For 3, 6 and 9 month analysis, n=10 per genotype per timepoint (exception, n=3 digenic animals). Statistical values were obtained by one-way ANOVA, followed by Tukey's multiple comparisons test (* P <0.05, ** P <0.01, *** P <0.001, **** P <0.0001); error bars indicate \pm SD.

Supp Fig 3



Supplemental Figure 3. Characterization of *Pkd1* mutant rats. (A) Analysis of observed animals born vs expected from *Pkd1*^{+/-} heterozygous crosses. No *Pkd1*^{-/-} animals were born. (B) Masson's Trichrome stain and MR imaging of kidneys from *Pkd1*^{+/-} rats aged to 3, 6, 9 and 12m. (C) Graphical representation of %KW/EHBW of *Pkhd1*^{+/-} at 12m compared to WT controls (n=4 vs 3, respectively). (D) Calculation of tubule-derived cystic burden as a fraction of total cystic burden for the digenic and *Pkd1*^{-/-} animals at P0 and P14. N represents the number of animals used in each analysis. (E-F) Graphical representation of BW and BUN measurements from 2w and 1m old animals. (E) No significant difference in BW was observed between the different genetic cohorts. (F) BUN levels were significantly higher in *Pkhd1*^{-/-};*Pkd1*^{+/-} plasma only at 1m. (G-H) Masson's Trichrome stain of representative liver sections from animals 1m old (G) and graphical analysis of LW/ERBW at 2w and 1m (H) showing no significant change in liver disease due to heterozygous loss of *Pkd1* in the *Pkhd1*^{-/-} background. Scale bar = 1000µm. Liver disease was not significantly worse due to the loss of *Pkd1* in *Pkhd1* null rats. Statistical values were obtained by Chi square analysis, Student's *T* test, or one-way ANOVA, followed by Tukey's multiple comparisons test where appropriate (**P* <0.05, ***P* <0.01, ****P* <0.001, *****P* <0.0001); error bars indicate ±SD.

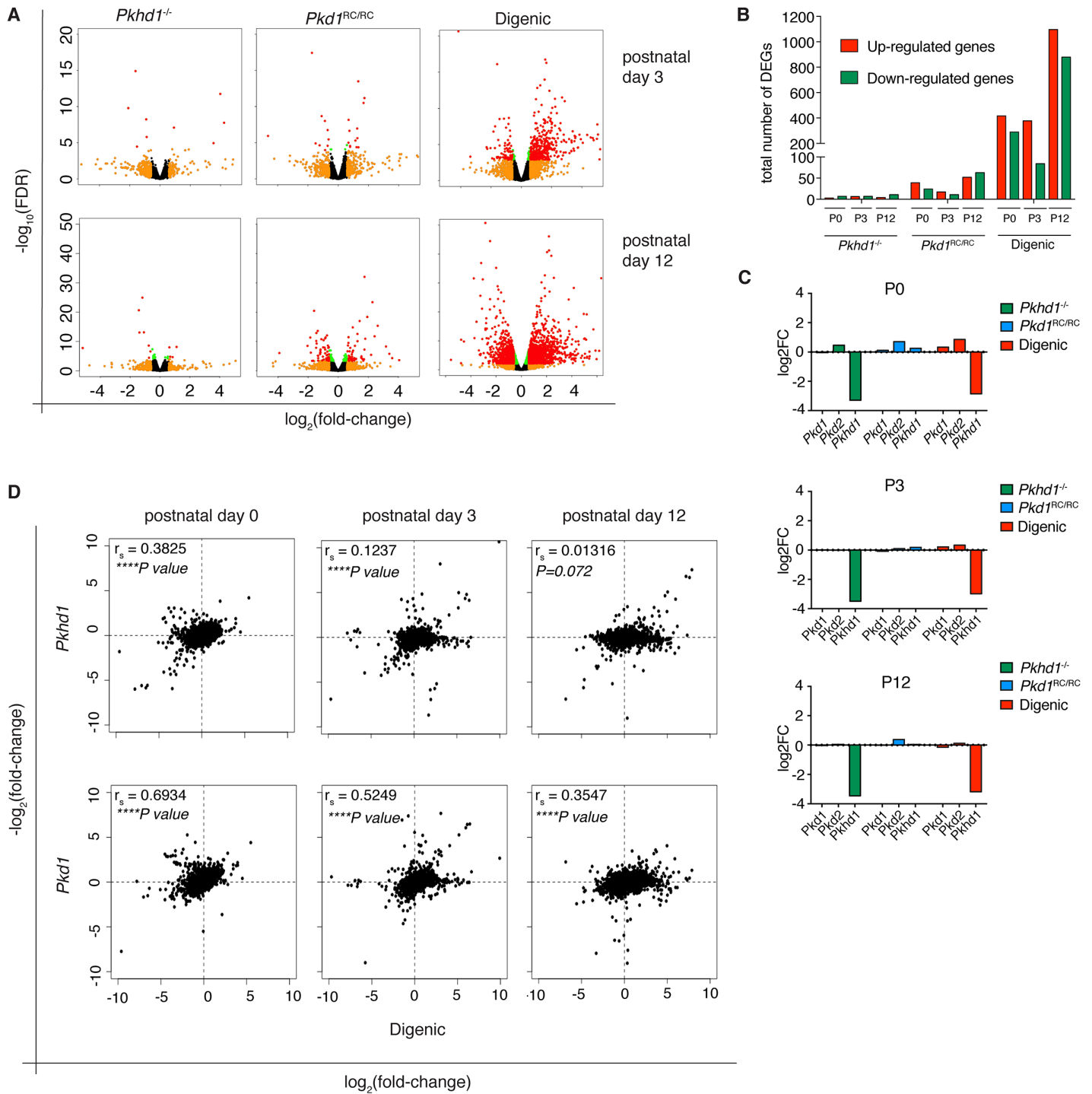
Supp Fig 4



Supplemental Figure 4. FPC expression and maturation is tightly regulated. (A) IB of endogenous FPC expression in two transformed human kidney epithelial cell lines and normal human kidney tissue using a huFPC antibody (clone ab11). FPC was only detectable in human kidney tissue. RCTE, renal cortical tubular epithelial; 5F, immortalized ADPKD-PKD1 patient kidney cell line; mp, membrane-prep; WCL, whole cell lysate. (B) FPC was not detected by western blot in immortalized *Pkhd1^{V5}* cells generated by crossing *Pkhd1^{V5/V5}* mice with the Immortomouse carrying the H-2Kb-tsa58 transgene allowing for interferon-inducible expression of generated cell lines¹, but PC1 is expressed. (C) Deglycosylation analysis in RCTE cell lysate transfected with N-terminal tagged SV5-Pk FPC construct. Exogenously expressed FPC did not recapitulate the maturation of endogenously expressed protein (see Figure 3D). (D) IB of lysate from *Pkhd1^{-/-}* (null) or *Pkhd1^{V5}* (V5) cultured cells showing V5 antibody specificity. (E) Quantification of total cells (DAPI) that had detectable primary cilia (Ac. tubulin) in

cultured *Pkhd1*^{-/-} (null) or *Pkhd1*^{V5} (V5) primary cells (see Figure 3E for IF image). Counts: null, 411 cilia in 770 total cells (53.4%); V5, 486 cilia in 953 total cells (51%). No significant difference was observed, 2-tailed Fisher's exact test.

Supp Fig 5



Supplemental Figure 5. Additional analysis of DEG profiles and Gene Set Enrichment Analysis (GSEA).

(A) Volcano plots of DEGs in *Pkhd1^{-/-}*, *Pkd1^{RC/RC}* and digenic kidneys at P3 and P12. Red denotes $\log_2\text{FC} \geq 0.585$ and $-\log_{10}\text{FDR} \geq 1.3$; orange, $\log_2\text{FC} \geq 0.585$ only; green, $-\log_{10}\text{FDR} \geq 1.3$ only. (B) Bar graph showing number of up- and down-regulated genes reaching significance ($\log_2\text{FC} \geq 0.585$ and $-\log_{10}\text{FDR} \geq 1.3$) in *Pkhd1^{-/-}*, *Pkd1^{RC/RC}* or digenic kidneys at P0, P3 and P12. Note at P12, there is a substantial increase in the number of DEGs in

digenic kidneys, likely due to secondary effects of cystogenesis. (C) RNA-seq data of *Pkd1*, *Pkd2* and *Pkhd1* expression in *Pkhd1*^{-/-} (green) *Pkd1*^{RC/RC} (blue) and digenic (red) kidneys at P0, P3 and P12. Only *Pkhd1* expression is significantly (FDR≤0.05) downregulated in both *Pkhd1*^{-/-} and digenic mutant kidneys. (D) Scatterplots of homozygous compared to digenic kidney expression profiles (each normalized to WT controls) at P0, P3, and P12. Spearman's rank coefficient (r_s) and (P values) are noted in top left corner of each plot. Pairwise comparisons indicate that expression profiles most strongly correlate at P0 relative to P3 and P12.

Supplemental Table 1. Renal Analysis of sexual dimorphism

Age		Female, Pkh^{d1}^{-/-}	Male, Pkh^{d1}^{-/-}	Female, Pkd1^{RC/RC}	Male, Pkd1^{RC/RC}	Female, digenic	Male, digenic
P0	Number of values	5	5	5	5	5	5
	Mean	1.052	1.076	1.386	1.478	2.636	2.746
	Std. Deviation	0.1244	0.0695	0.2207	0.1224	0.5391	0.536
	P value (Female vs Male)	0.7162		0.4386		0.7546	
P12	Number of values	5	5	5	5	5	5
	Mean	1.314	1.188	1.66	1.72	4.998	5.386
	Std. Deviation	0.03912	0.08927	0.07649	0.1744	0.6371	1.106
	P value (Female vs Male)	0.0202		0.501		0.5159	
P90	Number of values	5	5	5	5		
	Mean	1.504	1.418	1.9	1.914		
	Std. Deviation	0.1616	0.06301	0.1427	0.08385		
	P value (Female vs Male)	0.2999		0.8547			

Supplemental Table 2. Animals used for RNAseq

General ID	Pkhd1 genotype	Pkd1 genotype	Gender	Age (day)	BW	KW	%KW/BW	ng/uL	A260/A280
MFC-375	WT	WT	F	0	1391	14	1.01	309	2.08
MFC-383	WT	WT	M	0	1746	14	0.80	252	2.07
MFC-409	WT	WT	F	0	1252	13	1.04	99	2.09
MFC-387	-/-	WT	M	0	1231	14	1.14	172	2.08
MFC-394	-/-	WT	M	0	1357	15	1.11	217	2.09
MFC-399	-/-	WT	F	0	1275	13	1.02	306	2.09
MFC-360	WT	RC/RC	F	0	1393	22	1.58	379	2.08
MFC-365	WT	RC/RC	F	0	1448	18	1.24	325	2.07
MFC-397	WT	RC/RC	M	0	1626	27	1.66	558	2.09
MFC-369	-/-	RC/RC	M	0	1251	35	2.80	321	2.09
MFC-379	-/-	RC/RC	F	0	1284	46	3.58	692	2.07
MFC-381	-/-	RC/RC	M	0	1258	31	2.46	407	2.07
MFC-286	WT	WT	M	3.5	1672	22	1.32	585	2.11
MFC-324	WT	WT	M	3.5	2080	26	1.25	482	2.13
MFC-359	WT	WT	F	3.5	2152	20	0.93	785	2.09
MFC-223	-/-	WT	M	3.5	1943	28	1.44	395	2.12
MFC-300	-/-	WT	M	3.5	2099	26	1.24	639	2.11
MFC-319	-/-	WT	M	3.5	2258	25	1.11	512	2.11
MFC-281	WT	RC/RC	M	3.5	1715	29	1.69	572	2.13
MFC-282	WT	RC/RC	M	3.5	1786	29	1.62	572	2.12
MFC-326	WT	RC/RC	M	3.5	1929	33	1.71	727	2.08
MFC-305	-/-	RC/RC	F	3.5	1956	53	2.71	1161	2.11
MFC-316	-/-	RC/RC	F	3.5	1664	44	2.64	590	2.07
MFC-355	-/-	RC/RC	F	3.5	1732	60	3.46	733	2.07
MFC-262	WT	WT	M	12	6176	72	1.17	765	2.07
MFC-343	WT	WT	F	12	7570	97	1.28	618	2.1
MFC-344	WT	WT	M	12	7158	88	1.23	767	2.04
MFC-245	-/-	WT	F	12	7219	101	1.40	843	2.06
MFC-246	-/-	WT	F	12	7679	99	1.29	827	2.07
MFC-339	-/-	WT	M	12	7983	102	1.28	786	2.07
MFC-254	WT	RC/RC	M	12	6630	124	1.87	950	2.03
MFC-333	WT	RC/RC	M	12	4690	75	1.60	697	2.05
MFC-356	WT	RC/RC	M	12	3948	65	1.65	646	2.07
MFC-225	-/-	RC/RC	M	12	2945	195	6.62	877	2.04
MFC-250	-/-	RC/RC	M	12	2829	150	5.30	642	2.05
MFC-251	-/-	RC/RC	F	12	2699	132	4.89	630	2.09

Supplemental Table 4. Pkhd1^{-/-}, Pkd1RC/RC and digenic GSEA**Pkhd1^{-/-} GSEA**

GO term	Description	P-value	FDR q-value	Enrichment (N, B, n, b)	Genes (b)
GO:1905515	non-motile cilium assembly	9.80E-08	1.44E-03	8.54 (15192,44,485,12)	Ift80 - intraflagellar transport 80
GO:0060271	cilium assembly	8.89E-07	6.52E-03	2.38 (15192,174,1465,40)	Ift81 - intraflagellar transport 81
GO:0006700	C21-steroid hormone biosynthetic process	9.84E-07	4.81E-03	217.03 (15192,6,35,3)	polypeptide 1
GO:0044782	cilium organization	1.18E-06	4.33E-03	2.24 (15192,183,1629,44)	Ift81 - intraflagellar transport 81
GO:0042446	hormone biosynthetic process	4.04E-06	1.18E-02	61.51 (15192,26,38,4)	polypeptide 1
GO:0009855	determination of bilateral symmetry	4.34E-06	1.06E-02	3.26 (15192,70,1465,22)	Dyx1c1 - dyslexia susceptibility 1 candidate 1
GO:0042445	hormone metabolic process	4.40E-06	9.23E-03	21.61 (15192,111,38,6)	polypeptide 1
GO:0009799	specification of symmetry	5.91E-06	1.08E-02	3.21 (15192,71,1465,22)	Dyx1c1 - dyslexia susceptibility 1 candidate 1
GO:0061512	protein localization to cilium	5.92E-06	9.64E-03	6.17 (15192,32,847,11)	Tmem107 - transmembrane protein 107
GO:0008207	C21-steroid hormone metabolic process	7.29E-06	1.07E-02	46.04 (15192,12,110,4)	c18

Pkd1RC/RC GSEA

GO term	Description	P-value	FDR q-value	Enrichment (N, B, n, b)	Genes (b)
GO:0006259	DNA metabolic process	3.69E-13	5.42E-09	2.37 (15192,585,1062,97)	Fanci - fanconi anemia, complementation group i
GO:0006996	organelle organization	5.25E-13	3.85E-09	1.68 (15192,1723,1043,199)	Hps5 - hermansky-pudlak syndrome 5 homolog
GO:0051276	chromosome organization	5.74E-13	2.81E-09	3.03 (15192,241,1146,55)	Smc4 - structural maintenance of chromosomes 4
GO:0030030	cell projection organization	4.51E-11	1.65E-07	2.10 (15192,728,932,94)	Dock10 - dedicator of cytokinesis 10
GO:0006281	DNA repair	1.35E-10	3.96E-07	2.47 (15192,382,1031,64)	Fanci - fanconi anemia, complementation group i
GO:0044782	cilium organization	4.20E-10	1.03E-06	2.69 (15192,183,1511,49)	receptor 2 (flamingo homolog, drosophila)
GO:0007017	microtubule-based process	7.87E-10	1.65E-06	1.90 (15192,501,1644,103)	receptor 2 (flamingo homolog, drosophila)
GO:0007610	behavior	8.24E-10	1.51E-06	1.91 (15192,490,1637,101)	Npas3 - neuronal pas domain protein 3
GO:0120036	plasma membrane bounded cell projection or	2.12E-09	3.46E-06	1.90 (15192,523,1513,99)	receptor 2 (flamingo homolog, drosophila)
GO:0006260	DNA replication	2.30E-09	3.37E-06	3.61 (15192,127,1061,32)	member a
GO:0060271	cilium assembly	2.48E-09	3.30E-06	2.66 (15192,174,1511,46)	Celsr2 - cadherin, egf lag seven-pass g-type
GO:1905515	non-motile cilium assembly	3.37E-09	4.11E-06	5.84 (15192,44,1064,18)	Disc1 - disrupted in schizophrenia 1
GO:0022402	cell cycle process	7.14E-09	8.06E-06	1.74 (15192,641,1650,121)	Fanci - fanconi anemia, complementation group i
GO:1903046	meiotic cell cycle process	7.45E-09	7.80E-06	3.35 (15192,127,1178,33)	Ankle1 - ankyrin repeat and lem domain containing
GO:0016043	cellular component organization	1.12E-08	1.09E-05	1.25 (15192,3874,1639,523)	Hps5 - hermansky-pudlak syndrome 5 homolog
GO:0032200	telomere organization	1.84E-08	1.69E-05	4.00 (15192,66,1381,24)	Obfc1 - oligonucleotide/oligosaccharide-binding fold
GO:0000723	telomere maintenance	1.84E-08	1.59E-05	4.00 (15192,66,1381,24)	Obfc1 - oligonucleotide/oligosaccharide-binding fold
GO:0032392	DNA geometric change	1.85E-08	1.51E-05	6.91 (15192,29,1062,14)	cerevisiae)
GO:0070192	chromosome organization involved in meiotic c	2.27E-08	1.75E-05	5.24 (15192,46,1135,18)	cerevisiae)
GO:0071103	DNA conformation change	3.65E-08	2.68E-05	4.69 (15192,61,1062,20)	cerevisiae)
GO:0071840	cellular component organization or biogenesis	6.36E-08	4.44E-05	1.24 (15192,3961,1639,528)	Hps5 - hermansky-pudlak syndrome 5 homolog
GO:0032508	DNA duplex unwinding	1.01E-07	6.73E-05	7.38 (15192,24,1029,12)	cerevisiae)

GO:0006270	DNA replication initiation	1.59E-07	1.02E-04	6.20 (15192,24,1328,13)	Pola1 - polymerase (dna directed), alpha 1
GO:0006974	cellular response to DNA damage stimulus	1.89E-07	1.15E-04	2.22 (15192,588,651,56)	Fanci - fanconi anemia, complementation group i
GO:0120031	plasma membrane bounded cell projection as:	4.64E-07	2.72E-04	2.12 (15192,256,1511,54)	receptor 2 (flamingo homolog, drosophila)
GO:0006302	double-strand break repair	6.51E-07	3.67E-04	2.67 (15192,136,1381,33)	cerevisiae)
GO:0120039	plasma membrane bounded cell projection mc	9.96E-07	5.41E-04	2.63 (15192,232,871,35)	Dock10 - dedicator of cytokinesis 10
GO:0030031	cell projection assembly	1.10E-06	5.74E-04	2.09 (15192,262,1469,53)	receptor 2 (flamingo homolog, drosophila)
GO:0048812	neuron projection morphogenesis	1.42E-06	7.18E-04	2.62 (15192,226,871,34)	Dock10 - dedicator of cytokinesis 10
GO:0048858	cell projection morphogenesis	1.64E-06	8.04E-04	2.58 (15192,237,871,35)	Dock10 - dedicator of cytokinesis 10
GO:0007626	locomotory behavior	1.77E-06	8.39E-04	2.25 (15192,173,1637,42)	membrane 2
GO:0061512	protein localization to cilium	2.42E-06	1.11E-03	5.95 (15192,32,957,12)	Ift140 - intraflagellar transport 140
GO:0006310	DNA recombination	2.61E-06	1.16E-03	2.43 (15192,148,1479,35)	Brca2 - breast cancer 2
GO:1903047	mitotic cell cycle process	3.19E-06	1.38E-03	1.78 (15192,387,1650,75)	Fanci - fanconi anemia, complementation group i
GO:0007049	cell cycle	3.21E-06	1.35E-03	2.14 (15192,662,535,50)	Hfm1 - hfm1, atp-dependent dna helicase homolog
GO:0000226	microtubule cytoskeleton organization	5.58E-06	2.27E-03	2.00 (15192,289,1392,53)	Dynl1b - dynein light chain tctex-type 1b
GO:0006694	steroid biosynthetic process	5.68E-06	2.25E-03	11.50 (15192,76,139,8)	polypeptide 1
GO:0045005	DNA-dependent DNA replication maintenance	5.69E-06	2.19E-03	4.39 (15192,30,1615,14)	Brca2 - breast cancer 2
GO:0051053	negative regulation of DNA metabolic process	6.46E-06	2.43E-03	2.61 (15192,122,1479,31)	cerevisiae)
GO:0007611	learning or memory	7.64E-06	2.80E-03	2.04 (15192,218,1603,47)	Ttk1 - tau tubulin kinase 1
GO:0007018	microtubule-based movement	8.16E-06	2.92E-03	4.82 (15192,207,213,14)	Dnah8 - dynein, axonemal, heavy chain 8
GO:0051656	establishment of organelle localization	8.46E-06	2.95E-03	2.26 (15192,251,1043,39)	Syt11 - synaptotagmin xi
GO:0051640	organelle localization	8.96E-06	3.05E-03	1.78 (15192,370,1618,70)	Ntn1 - netrin 1

Digenic GSEA

GO term	Description	P-value	FDR q-value	Enrichment (N, B, n, b)	Genes (b)
GO:0061512	protein localization to cilium	3.00E-06	2.09E-03	5.85 (15192,32,974,12)	Ift140 - intraflagellar transport 140
GO:1905515	non-motile cilium assembly	4.98E-06	3.04E-03	5.31 (15192,44,845,13)	Dync2h1 - dynein cytoplasmic 2 heavy chain 1
GO:0007368	determination of left/right symmetry	3.87E-06	2.47E-03	3.77 (15192,69,1111,19)	expression)
GO:0009855	determination of bilateral symmetry	5.09E-06	2.99E-03	3.71 (15192,70,1111,19)	expression)
GO:0009799	specification of symmetry	6.40E-06	3.24E-03	3.66 (15192,71,1111,19)	expression)
GO:0044782	cilium organization	2.33E-08	4.27E-05	2.84 (15192,183,1111,38)	receptor 2 (flamingo homolog, drosophila)
GO:0060271	cilium assembly	2.03E-07	2.98E-04	2.75 (15192,174,1111,35)	receptor 2 (flamingo homolog, drosophila)
GO:0010810	regulation of cell-substrate adhesion	8.59E-07	7.87E-04	2.55 (15192,178,1204,36)	Itga5 - integrin alpha 5 (fibronectin receptor alpha)
GO:0120031	plasma membrane bounded cell projection as:	1.65E-06	1.28E-03	2.30 (15192,256,1111,43)	receptor 2 (flamingo homolog, drosophila)
GO:0043547	positive regulation of GTPase activity	1.25E-06	1.08E-03	2.29 (15192,181,1542,42)	Tbc1d8b - tbc1 domain family, member 8b
GO:0000226	microtubule cytoskeleton organization	3.52E-10	1.72E-06	2.27 (15192,289,1598,69)	1
GO:0030031	cell projection assembly	3.29E-06	2.19E-03	2.24 (15192,262,1111,43)	receptor 2 (flamingo homolog, drosophila)
GO:0043087	regulation of GTPase activity	7.49E-07	7.33E-04	2.16 (15192,251,1428,51)	Tbc1d8b - tbc1 domain family, member 8b
GO:0070925	organelle assembly	1.47E-06	1.20E-03	2.11 (15192,389,979,53)	receptor 2 (flamingo homolog, drosophila)

GO:0032989	cellular component morphogenesis	5.66E-07	6.39E-04	2.05 (15192,430,1052,61)	receptor 2 (flamingo homolog, drosophila)
GO:0010769	regulation of cell morphogenesis involved in d	5.99E-06	3.25E-03	2.00 (15192,274,1439,52)	Ntn1 - netrin 1
GO:0051656	establishment of organelle localization	6.46E-06	3.16E-03	1.98 (15192,251,1589,52)	1
GO:0007017	microtubule-based process	3.62E-10	1.33E-06	1.94 (15192,501,1598,102)	receptor 2 (flamingo homolog, drosophila)
GO:0007010	cytoskeleton organization	1.37E-12	1.01E-08	1.91 (15192,651,1598,131)	1
GO:0030029	actin filament-based process	6.16E-06	3.23E-03	1.88 (15192,302,1632,61)	Bcar1 - breast cancer anti-estrogen resistance 1
GO:0120036	plasma membrane bounded cell projection or	1.45E-08	3.55E-05	1.83 (15192,523,1591,100)	receptor 2 (flamingo homolog, drosophila)
GO:0051493	regulation of cytoskeleton organization	7.08E-07	7.41E-04	1.79 (15192,444,1607,84)	1
GO:0030030	cell projection organization	1.45E-09	4.27E-06	1.76 (15192,728,1491,126)	receptor 2 (flamingo homolog, drosophila)
GO:0022402	cell cycle process	5.16E-06	2.91E-03	1.61 (15192,641,1527,104)	1
GO:0006928	movement of cell or subcellular component	1.78E-06	1.30E-03	1.57 (15192,957,1308,129)	receptor 2 (flamingo homolog, drosophila)
GO:0006996	organelle organization	2.74E-13	4.02E-09	1.53 (15192,1723,1637,284)	Myh14 - myosin, heavy polypeptide 14
GO:0033043	regulation of organelle organization	4.52E-07	6.02E-04	1.49 (15192,1084,1607,171)	1
GO:0051128	regulation of cellular component organization	1.72E-08	3.61E-05	1.40 (15192,2123,1394,273)	Ntn1 - netrin 1
GO:0016043	cellular component organization	5.65E-08	9.20E-05	1.24 (15192,3874,1602,508)	Hps5 - hermansky-pudlak syndrome 5 homolog
GO:0071840	cellular component organization or biogenesis	5.16E-07	6.31E-04	1.22 (15192,3961,1602,511)	Hps5 - hermansky-pudlak syndrome 5 homolog

Species used: Mus musculus

The system has recognized 16595 genes out of 18049 gene terms entered by the user.

16594 genes were recognized by gene symbol and 1 genes by other gene IDs .

63 duplicate genes were removed (keeping the highest ranking instance of each gene) leaving a total of 16532 genes.

Only 15192 of these genes are associated with a GO term.

[The GOrrilla database is periodically updated using the GO database and other sources.](#)

The GOrrilla database was last updated on Dec 23, 2017

P-value is the enrichment p-value computed according to the mHG model. This p-value is not corrected for multiple testing of 14663 GO terms.

FDR q-value is the correction of the above p-value for multiple testing using the Benjamini and Hochberg (1995) method.

Namely, for the i^{th} term (ranked according to p-value) the FDR q-value is $(p\text{-value} * \text{number of GO terms}) / i$.

Enrichment (N, B, n, b) is defined as follows:

N - is the total number of genes

B - is the total number of genes associated with a specific GO term

n - is the number of genes in the top of the user's input list or in the target set when appropriate

b - is the number of genes in the intersection

Enrichment = $(b/n) / (B/N)$

Supplemental Table 5. Merged annotated gene list extracted from GO:0044782, GO:0060271, GO:0061512, GO:1905515 using the Gene Ontology Consortium (<http://amigo.geneontology.org/amigo/>) gene

Foxj1	Tekt2	Tmem231	Csnk1d	Ube2b
Ttll1	Parva	Nme7	Atg5	Bbs5
Cep135	Trove2	Gorab	Ift20	Spata7
Bbs2	Ift74	Ubxn10	Tmem216	Hspb11
Ccp110	Rab23	Unc119b	Tmem138	Spef2
Cfap54	Asap1	Dzip1	Exoc5	Fam161a
Htt	Ift88	Vangl2	Ttll3	Dnah7c
Ablim1	Tmem107	Sept9	Arl6	Avil
Poc1a	Cep78	Kif24	Rsph4a	Mak
Rilp	Pcm1	2700049A03Rik	Tekt5	
Kif17	Rab29	Ccdc103	Dnaic2	
Rfx2	Ift22	E2f4	Tulp1	
Dnm2	Kif27	Cluap1	Iqcg	
Ift81	Dnaic1	Kctd17	Ttc30b	
Kif3a	Arhgap35	Fnbp11	Arf4	
Pcnt	Snx10	Snap29	Wwtr1	
Map4	Mkks	Atmin	Bbs1	
Stil	Ptpn23	Ccdc28b	Tub	
Traf3ip1	Tmem80	Cyld	Gsn	
Rpgr	Wdpcp	1810043G02Rik	Tmem67	
Spag16	Tulp4	Tctn3	Ick	
Ift80	Pibf1	Ift43	Lztf1	
Spag17	Dnah1	Actr3	Ift57	
Tmem237	Cep97	Ttc17	Ttc30a1	
Poc1b	Odf2	Rab8a	Rilp2	
Cep83	Rilp1	Bbs10	Zmynd10	
Rab17	Bbs12	Cfap20	Nme5	
Cby1	Dnaaf1	Tulp2	Bbip1	
Wdr60	Gas8	Ablim3	Ttc26	
Evi5l	Tctn1	B9d2	Dync2li1	
Dyx1c1	Pqbp1	Tmem141	Ttc30a2	
Ocl	Spata6	Ptpdc1	Wdr5	
Cenpj	Ssx2ip	Ift46	Arl13b	
Ehd1	Dnaaf2	Ccdc39	Mks1	
Lrguk	Ift52	Eno4	Fopnl	
Dnah12	Rab3ip	Vdac3	Trim59	
Dctn1	Klc3	Fuz	Ak7	
Ccdc114	Actr2	Tctn2	Wdr5b	
Wrap73	Tbc1d7	Nudcd3	Arl3	
Ttbk2	Tulp3	Tctex1d2	Tekt1	
Neur1a	Lca5	Tpgs1	Tap1	
Cep120	Ehd3	Wdr34	Rsph9	
Dnal1	Hap1	Dynll2	Cdc14a	
Ift27	Atg3	Intu	Tmem17	
Ahi1	Ssna1	Dnah5	Adamts16	
Ofd1	Tbc1d30	Bbs4	Ulk4	
Rabl2	Sept2	Dnhd1	Fam92a	
Sept7	Gm20695	Efcab7	Iqcb1	
Rsph1	Ccdc151	Tchp	Ccdc183	
Cep89	Atxn10	Atp6v1d	B9d1	